Properties of the Dominant Inter-Area Modes in the WECC Interconnect

Dan Trudnowski
Montana Tech, Butte, MT
dtrudnowski@mtech.edu
Jan. 16, 2012

***Abstract*—Because of the long transmission paths in the WECC interconnect, electromechanical small-signal stability is of concern. The system contains several modes of oscillation. Two of these modes are especially wide-spread while the others tend to be more localized. This paper describes the properties of these modes based upon the latest available information and data. These properties include the modal frequencies, damping, shape, interaction paths, and participation factors.**

I. Nomenclature

BC = British Columbia, Canada.
BPA = Bonneville Power Administration.
COI = California-Oregon intertie (a critical transmission intertie).
PDCI = Pacific DC Intertie (a major DC transmission line from northern Oregon to southern California).
PSS = power system stabilizer.
PMU = phasor measurement unit.
HVDC = high voltage direct current.
US = United States of America.
WAMS = wide area measurement system.
WECC = Western Electricity Coordinating Council.
wNAPS = western North American power system.

II. Introduction

POWER system electromechanical oscillatory behavior is an inherent characteristic of the synchronous machines that are interconnected via transmission systems. As more power is transferred over longer distances, these oscillations can become less damped and thus the primary stability limit. The wNAPS, which extends over the entire western US and Canada, includes very long transmission paths resulting in significant inter-area oscillations. Oscillatory stability has historically been, and continues to be, a concern of the wNAPS. Several oscillatory events occur each year. The large majority of these are well damped; but, some are not. Related to recent history, the most infamous event was unstable and resulted in the system break up in 1996 [1].

The purpose of this paper is to provide a summary of the interarea modal properties of the wNAPS with a focus on the two most wide-spread inter-area modes. These properties are primarily calculated from actual-system measurements over a long period. The reader is referred to [2] for information on the measurement-based analysis techniques. Also, some model-based analyses are employed.

This work was supported by the BPA under contract 37508 and by the US Department of Energy under contract DE-FC26-06NT42750.

Electromechanical modes are defined by the following terms. The reader is referred to Appendix 1 for a short theoretical discussion of these terms. For more detailed information on the topic, I recommend [3].

- **Mode frequency**: The frequency at which a given mode oscillates (typically in Hz).
- **Mode damping**: A measure of how long it takes for a given mode to dissipate in a transient. Typically measured in %D where %D = 100*(damping ratio). Note, 1/(damping ratio) ≅ the number of cycles of an oscillation before the oscillation completely dissipates.
- **Observability**: The content of a given mode in a given measured signal.
- **Mode Shape**: A measure of the observability of a given mode. Mode shape is a complex number and is associated with a given mode and system state (e.g., generator speed). The amplitude of the shape is a measure of the magnitude of the state variable in the modal oscillations. The angle of the shape is a measure of the phase of the state variable in the modal oscillations.
- **Controllability**: The extent to which a given mode can be damped from control of a given actuator at a given location in the grid.
- **Participation Factor**: A measure of controllability of a given mode at a given location (typically a generator). The participation factor is a direct measure of how much damping a PSS unit at a given generator can dampen an oscillation of a give mode.
- **Modal Interaction**: Loosely defined as a measure of modal energy exchange between different areas of a system. For example, if two areas swing against each other at a given mode, modal energy is exchanged through one or more transmission lines. Interaction is a measure of modal energy being exchanged on a given line.
- **Modal Excitability**: Loosely defined to be a measure of how much a given contingency excites an oscillation containing a given mode.

Based upon nearly 30 years of continuous engineering analyses, the oscillatory properties of the wNAPS are fairly well known. The majority of the analyses are based on signal processing of actual-system measurements ([5] thru [10]). Most recently, these have been periodic PDCI probing tests and Chief-Jo brake pulses conducted throughout the summer seasons of 2009, 2011, and 2012 ([9] and [10]). The PMU

measurement coverage of the 2012 tests was considerably wider than the 2009/2011 tests and represents the best coverage to date. A total of 26 tests were conducted in 2012. For the 2009 and 2011 tests, PMU coverage was limited to the BPA area and a total of 30 tests were conducted. The test analyses have provided rich knowledge on the modal frequencies, damping, and shape. Modal controllability properties are less known and are based upon model studies.

The wNAPS contains four well-known inter-area modes of interest.

- "NS Mode A" nominally near 0.25 Hz. This was historically termed the "NS Mode."
- "NS Mode B" nominally near 0.4 Hz. This was historically termed the "Alberta Mode."
- "BC" mode nominally near 0.6 Hz; and,
- "Montana" mode nominally near 0.8 Hz.

Other modes exist in the system; but, these four have been observed the most and are well understood. Two other inter-area modes, mostly in the southern half of the system, typically occur near 0.5 Hz and 0.7 Hz. Of the four modes, NS Modes A and B are the most widespread and troublesome. And, they are the primary focus of this paper.

III. NS Mode A

NS Mode A is the lowest frequency mode in the wNAPS. The following summarizes the modes properties when the system is operating under normal conditions. Today, its frequency is typically near 0.25 Hz. During the past three years, its damping has consistently been near 10% or more during the summer season. NS Mode A has the northern half of the wNAPS swinging against the southern half. By far the most dominant observability point is the Alberta Canada area of the system. One might conclude that this mode is actually Alberta oscillating against the rest of the system. Model-based controllability studies outlined below indicate that the only way to dampen the NS Mode A is from Alberta.

Fig. 1 shows the mode estimates for a typical summer day. Note the diurnal variation in the mode frequency. It is typical and expected that the mode frequency increases during the lighter loading time of the night. The mode damping stays fairly constant in the 10% to 15% range. The faster variations in the damping are typical of random variations in the estimator algorithm. That is, when damping is high, the algorithm cannot exactly estimate the mode damping.

The mode-shape estimates from the 2009 thru 2012 probe tests are very consistent. The Aug. 23, 2012 B tests represents the widest coverage mode-shape estimates to date. Fig. 2 and Fig. 3 show the mode shape for selected PMUs across the system. The reader is referred to [10] for a more detailed list of mode shapes. Note the two PMUs in Alberta (GN01 and LA01) have a much larger magnitude. GN01 is further north and is hypothesized to be near the center for the northern mass of the mode. The node or dividing line for the mode is north of Tesla and very close to Malin.

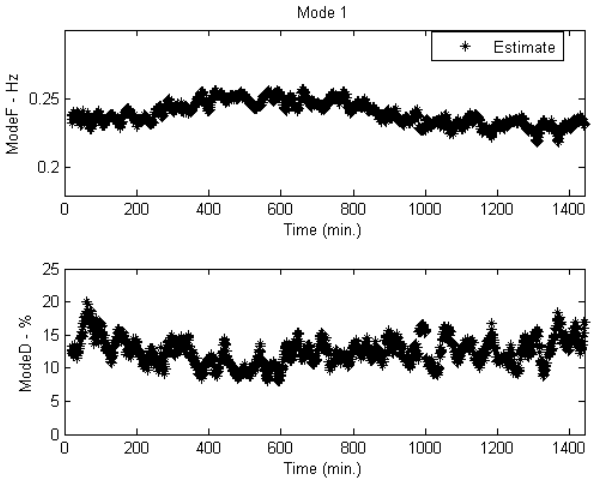

Fig. 1: NS Mode A estimates for May 29, 2012. Plot starts at midnight GMT (5:00 pm PDT).

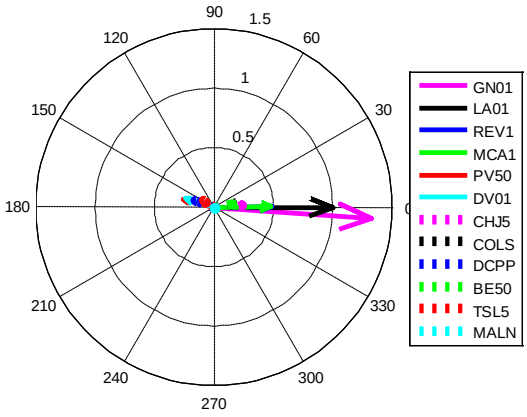

Fig. 2: NS Mode A shape estimated during the Aug. 23, 2012 PDCI probing test B. GN01 = Genesee (Alberta), LA01 = Langdon (Alberta), REV1 = Revelstoke (BC), MCA1 = Mica (BC), COLS = Colstrip (MT), CHJ5 = Chief Jo (WA), BE50 = Big Eddy (OR), MALN (OR-CA), TSL5 (Mid CA), DCPP (So. CA), DV01 = Devers (So. CA), PV50 = Palo Verde (AZ). Alberta connected.

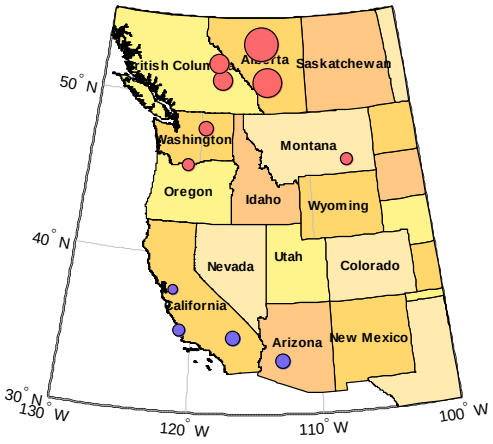

Fig. 3: Map of NS Mode A shape from Fig. 2. Red circles oscillate against blue; circle diameter is proportional to mode-shape magnitude. Alberta connected.

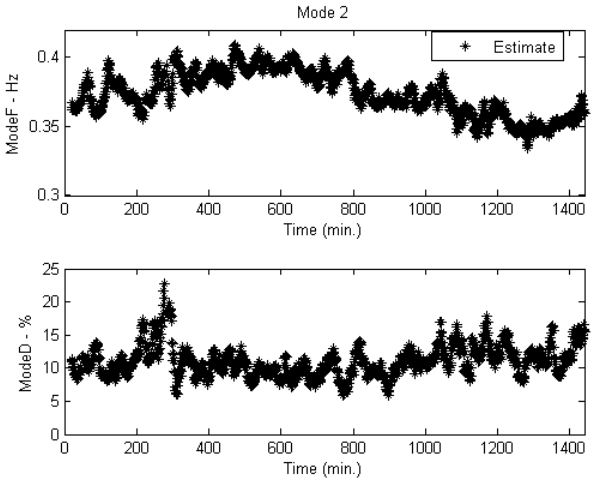

Fig. 4: NS Mode B estimates for May 29, 2012. Plot starts at midnight GMT (5:00 pm PDT).

IV. NS Mode B

NS Mode B first showed up after Alberta interconnected to the system [5] and has a very widespread shape. Under normal operating conditions, the mode frequency varies from 0.34 Hz to 0.4 Hz. Recently during heaving loading, the damping is typically between 5% and 10%. It has the Alberta area swinging against BC and the northern US which in turn swings against the southern part of the US. The northern node or dividing line is just south of Langdon on the BC/Alberta intertie. The other node is typically south of Tesla and north if Diablo Canyon. The observability is much more widespread than NS Mode A in that no one location is dominant.

Fig. 4 shows the mode estimates for a typical summer day. Note the diurnal variation in the mode frequency which is significantly more than NS Mode A. It is typical and expected that the mode frequency increases during the lighter loading time of the night. The mode damping slightly drops during the early morning hours. The faster variations in the damping are typical of random variations in the estimator algorithm. That is, when damping is high, the algorithm cannot exactly estimate the mode damping.

As with NS Mode A, the mode-shape estimates from the 2009 thru 2012 probe tests are very consistent. The Aug. 23, 2012 B tests represents the widest coverage mode-shape estimates to date. Fig. 5 and Fig. 6 show the NS Mode B shape for the same selected PMUs as shown previously for NS Mode A. Again, the reader is referred to [10] for more detailed mode-shape data. Note that the largest amplitude is located at GN01 (Genesee in Alberta). The amplitude at Langdon in Alberta is zero (too small to accurately estimate). This is likely because Langdon is at a node of the mode (i.e., a dividing line). Note that PV50 and DV01 in the southern part of the wNAPS swing in phase with GN01. Also, note the relatively large magnitude of the mode throughout the system. The other node or dividing line for the mode is just south of Tesla.

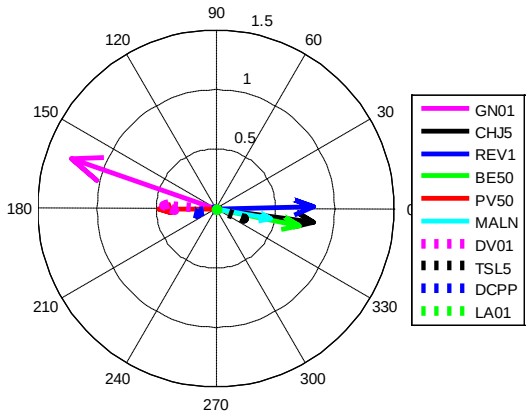

Fig. 5: NS Mode B shape estimated during the Aug. 23, 2012 PDCI probing test B. GN01 = Genesee (Alberta), LA01 = Langdon (Alberta), REV1 = Revelstoke (BC), MCA1 = Mica (BC), COLS = Colstrip (MT), CHJ5 = Chief Jo (WA), BE50 = Big Eddy (OR), MALN (OR-CA), TSL5 (Mid CA), DCPP (So. CA), DV01 = Devers (So. CA), PV50 = Palo Verde (AZ). Alberta Connected.

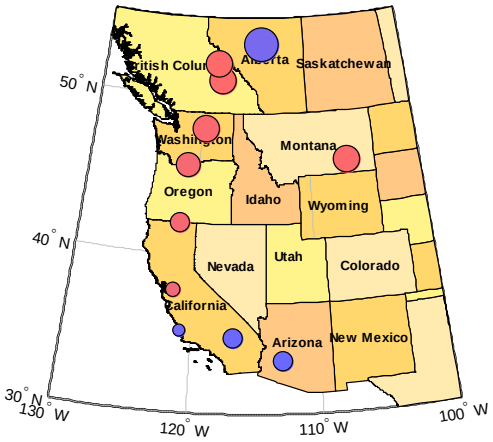

Fig. 6: Map of NS Mode B shape from Fig. 5. Red circles oscillate against blue; circle diameter is proportional to mode-shape magnitude. Alberta Connected.

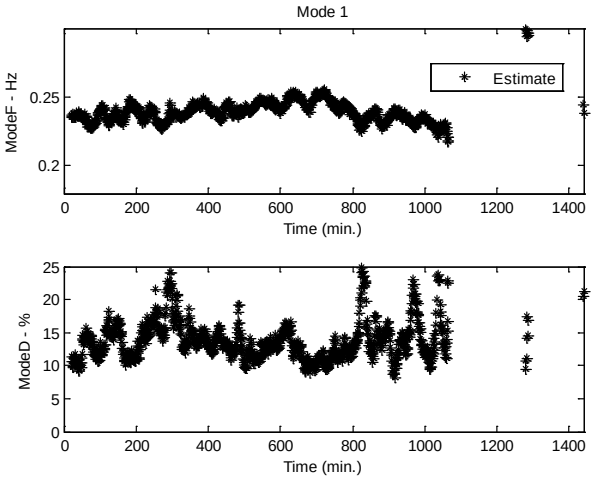

Fig. 7: NS Mode A estimates for June 18, 2012. Plot starts at midnight GMT (5:00 pm PDT). Alberta disconnects just prior to the 1100 min. point.

V. NS Modes And the Alberta Connection

Historically, the Alberta interconnection has the strongest influence on NS Modes A and B. With Alberta connected, Mode B typically has the lowest damping. Its damping appears to be influenced by several intertie flows, including: the COI flows, the Alberta to BC flows, and Montana to Washington flows. With Alberta disconnected, Modes A and B melt into a single north-south mode nominally near 0.32 Hz which again has a dividing line near the COI. This mode is typically more lightly damped than with Alberta connected.

The modal estimates for a typical Alberta disconnect are shown in Fig. 7 and Fig. 8. The modes are estimated with an automated mode meter. The disconnect occurs just prior to the 1100 min. point. Note that Mode A disappears and Mode B suddenly drops in frequency and the damping slightly decreases. This is a typical response. The mode shape of the NS Mode B with Alberta disconnected is very similar to NS Mode B with Alberta except for the Alberta PMUs are not included.

An interesting condition occurred Sep. 13, 2012 during probing tests. For this day, the 500-kV connection to Alberta was open-circuited; but, Alberta remained connected via the lower voltage sub-transmission. This represents a very weak connection between BC and Alberta. The same PMUs used for the analyses in sections III and IV, although, the GN01, DCPP, and TSL5 PMUs were not available.

The NS mode A dropped to 0.18 Hz and the NS Mode B dropped to 0.32 Hz. Fig. 9 thru Fig. 12 show the mode shapes. The observability of the NS Mode A in Fig. 9 and Fig. 10 is very much dominated by Alberta as indicated by the magnitude of the mode shape. The magnitude is more than 10 times larger in Alberta than any other area. This indicates that the mode has Alberta oscillating against the system more as a local mode.

The mode shape of the NS Mode B is shown in Fig. 11 and Fig. 12. It is very similar to the shape with Alberta fully connected.

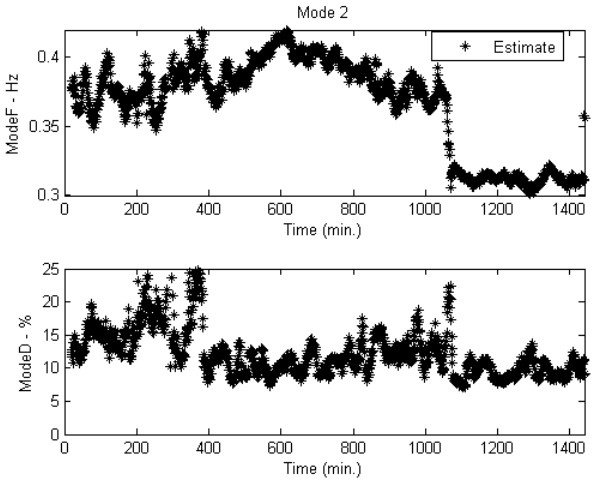

Fig. 8: NS Mode B estimates for June 18, 2012. Plot starts at midnight GMT (5:00 pm PDT). Alberta disconnects just prior to the 1100 min. point.

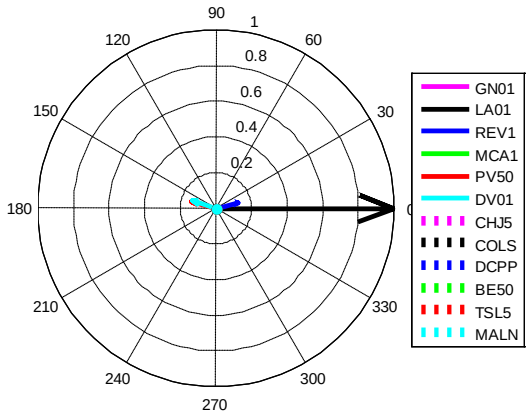

Fig. 9: NS Mode A shape estimated during the Sep. 13, 2012 PDCI probing test B. GN01 = Genesee (Alberta), LA01 = Langdon (Alberta), REV1 = Revelstoke (BC), MCA1 = Mica (BC), COLS = Colstrip (MT), CHJ5 = Chief Jo (WA), BE50 = Big Eddy (OR), MALN (CA-OR), TSL5 (Mid CA), DCPP (So. CA), DV01 = Devers (So. CA), PV50 = Palo Verde (AZ). NOTE:

GN01, MCA1, DCPP, and TSL5 were not available for analyses. Alberta weakly connected.

Fig. 10: Map of NS Mode A shape from Fig. 9. Red circles oscillate against blue; circle diameter is proportional to mode-shape magnitude. Alberta weakly connected.

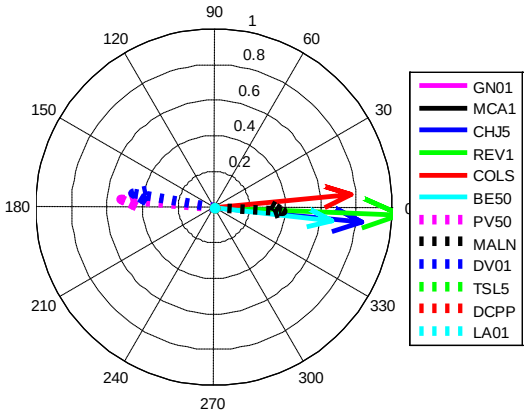

Fig. 11: NS Mode B shape estimated during the Sep. 13, 2012 PDCI probing test B. GN01 = Genesee (Alberta), LA01 = Langdon (Alberta), REV1 = Revelstoke (BC), MCA1 = Mica (BC), COLS = Colstrip (MT), CHJ5 = Chief Jo (WA), BE50 = Big Eddy (OR), MALN (OR-CA), TSL5 (Mid CA), DCPP (So. CA), DV01 = Devers (So. CA), PV50 = Palo Verde (AZ). NOTE: GN01, MCA1, DCPP, and TSL5 were not available for analyses. Alberta weakly connected.

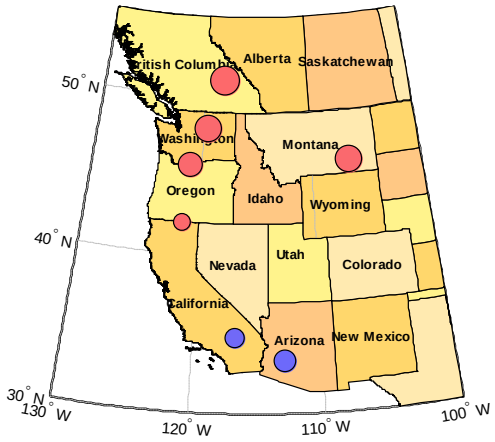

Fig. 12: Map of NS Mode B shape from Fig. 11. NOTE: GN01 was not available for analyses. Red circles oscillate against blue; circle diameter is proportional to mode-shape magnitude. Alberta weakly connected.

VI. The Other Modes

The "BC" mode primarily has the BC area swinging against the rest of the system. The "Montana" mode has Montana oscillating against the rest of the system. Although these two modes are more localized; they do ripple through the system at a high enough energy to cause concern.

VII. Relative Observability, Energy and Interactions

The above discussion provides an overview of the individual modes. The goal of the following is to provide perspective on the observability of the modes relative to each other, and the interactions of the modes. Modal interaction is loosely defined to be a measure of modal energy exchange for a given mode between different areas of a system. A good way to view the interactions is via spectral plots.

Fig. 13 through Fig. 18 show the estimated Power Spectral Densities (PSDs) of the FreqLFD signal at Genesee (Alberta), Mica (BC), Colstrip (MT), Chief Jo (WA), Big Eddy (OR), and Palo Verde (AZ) during the Aug. 23, 2012 probing tests. FreqLFD is the estimated frequency at a PMU calculated by taking the numerical derivative of the voltage phase angle. Each spectrum is shown for two data sets: "ambient" is when the PDCI probing is turned off; and "probing" for when the probing is turned on.

First, consider the ambient conditions. Each plot reveals considerable information about the relative observability of each mode. As an example, consider Fig. 13. The large peak near 0.24 Hz tells us that the Genesee power plant has very large observability for the NS Mode A. The smaller peak near 0.35 Hz tells us that the Genesee swings considerably less at the NS Mode B compared to NS Mode A. Mode A tends to have larger observability than Mode B at Genesee, Mica, and Palo Verde. And, NS Mode B is more observable at Colstrip, Chief Jo, and Big Eddy.

Fig. 19 thru Fig. 23 show the spectrums of the MW flows on major interties. These plots provide information on the interaction between areas. Fig. 20 specifically shows a time

frequency plot over an entire typical day for Malin-Round Mountain 1. Surprisingly, NS Mode A tends to have higher energy in all the interaction spectrums than NS Mode B. Also, Colstrip MW has very low interaction energy at both NS modes (Fig. 21); but, the FreqLFD at Colstrip in Fig. 15 does show energy. This inconsistency is unexpected.

At this point, one should NOT conclude that the NS Mode A dominates a contingency response. In fact, the following discussion will argue that actually NS Mode B dominates the response to most contingencies. All one can conclude is that NS Mode A is highly observable in the AMBIENT interactions.

VIII. Modal Controllability and Excitability

Controllability analysis tells us the locations where control systems are effective to dampen a give mode. Excitability is related to controllability; it is a measure of contingencies that will excite a mode. Only limited controllability and excitability information can be extracted from actual-system measurements. Therefore, model studies are also needed.

While model studies are needed to fully comprehend controllability, the PDCI modulation tests do provide information on the ability of PDCI modulation to dampen oscillations. In each Fig. 13 thru Fig. 18 plot, the NS Mode A peak increases very little during probing. This tells us that the mode is NOT controllable from PDCI modulation. But, the NS Mode B energy near 0.35 Hz does significantly increase with probing. Therefore, this mode is very controllable from PDCI modulation. More detailed correlation analysis using coherency plots present in [10] further verifies this conclusion.

A. The MiniWECC Model Controllability

Detailed controllability analysis requires linear models of the system. Two approaches are typical. With the first, a full-order transient stability model is linearized using one of a few commercial software packages specifically designed for power systems. The resulting linear model is very high order and requires specialized numerics to conduct eigenanalysis and other calculations. The 2nd approach involves reducing the order of the nonlinear model to a reasonable size and then linearizing. With a smaller linear model, modern control-design computing tools such as Matlab® can be utilized.

Our experience with the first approach has been frustrating at best. The large order of the linear model is very cumbersome and limiting! We prefer to use, and did use, the 2nd approach. The key advantage is that we have full access to the wide-range and highly detailed linear analysis tools available with Matlab®. We designed the reduced-order model to represent the overall inter-area modal properties and have enough complexity of the full-size system to accurately evaluate potential system-wide damping control technologies.

We term our reduced-order model the "miniWECC" model; it is shown in Fig. 24. A description of the model derivation is contained in [11] and [12]. The derivation consisted of reducing a full-sized model using generator equivalencing and combining transmission paths. The system contains 34 generators, 122 buses, 171 lines and transformers, 19 load buses, and two DC lines. The model was realized and tested in two power-system analysis programs: GE Energy's Positive Sequence Load Flow (PSLF) and the Matlab® Power Systems Toolbox (PST) which is available with the book [3]. It includes power flow, transient simulation, and full linearization functions. Highly detailed generator models are used in the model and comparisons between PSLF and PST match closely [11].

Seven power flow cases representing a wide-range of operating conditions are used in the miniWECC model. Modal analysis was conducted for each power flow case, including examining: the mode variations for different power flow conditions; variations of participation factors; and, examination of mode shape [12]. The following summarizes the analyses.

The inter-area modes for 7 power-flow cases are contained in Table 1. The four previously described modes seen in the actual system are contained in the model. In addition, the model has two other modes that are suspected to exist in the actual system but are less understood. The E-W 1 mode has the southwest swinging against the southeast. The E-W 2 mode also ripples through the southern half of the system.

Note the variation in the modes; especially the NS Mode A and NS Mode B which are unstable for many of the power-flow cases. With Alberta disconnected, these two modes combine into a single mode as reflected in power-flow case 2. The general shapes of the modes are very consistent and very closely match the actual system. Many variations of the power-flow cases were studied to determine what loading conditions affect the damping of the modes.

The participation factors are a direct measure of controllability of a given mode at a given location. At a given generator, the participation factor is a direct measure of how much damping a PSS unit can dampen an oscillation of a given mode. As an example, the participation factors for power flow case 4 are shown in Fig. 25. For NS Mode A, the participation factor at generator 34 (Alberta) is nearly 10 times larger than any other generator indicating the mode is easily damped from generator 34. Mode B's participation factors are very wide-spread with no one area dominating. The locations with the largest participation factors are the Pacific Northwest US, northern Canada, and the deep south.

B. Modal Excitability

The miniWECC participation factors and the PDCI probing spectrums in Fig. 13 thru Fig. 23 also provide evidence on the excitability of the modes. Because NS Mode A is uncontrollable from any location except Alberta (as evidence from the miniWECC model), one can hypothesize that only contingencies involving the Alberta area will significantly excite the mode. Similarly, nearly all major contingencies excite NS Mode B because its controllability is much more widespread.

One can test the hypotheses on Prony analysis of actual-system events. When conducting Prony analysis, a good signal for estimating the modes is the Big Eddy – Malin

FreqLFD Hz. The ambient spectrum of this signal is shown in Fig. 26 for the Aug. 23, 2012 probe test. Note that both NS Modes are present in the signal. And, NS Mode A has a larger spectral peak than NS Mode B.

The first such event is a Chief Jo brake pulse. Fig. 27 shows the response of the Big Eddy – Malin signal, and Fig. 28 shows the response of the Malin – Round M. 1 MW to a brake pulse on Sep. 15, 2011. The Prony results are shown in Table 2. Three modes were estimated in the Prony analysis – NS Modes A and B, and the BC Mode. These three modes make up the "Prony" response in Fig. 27 and Fig. 28. Table 2 shows the amplitudes of the modes estimated by the Prony analysis. Note that NS Mode B is approximately 3 times larger than NS Mode A for both signals. This is despite the fact that NS Mode A is much more observable in the ambient (as indicated by Fig. 19, Fig. 20, and Fig. 26). This indicates that a Chief-Jo brake pulse excites the NS Mode B much more than NS Mode A.

A second contingency example is from a Palo Verde trip on July 4, 2012. The system response and Prony results for NS Modes A and B are shown in Fig. 29, Fig. 30, and Table 3. In this case, NS Mode B's amplitude is more than double the amplitude of NS Mode A. The conclusion is that the Palo Verde event excites the NS Mode B much more than NS Mode A.

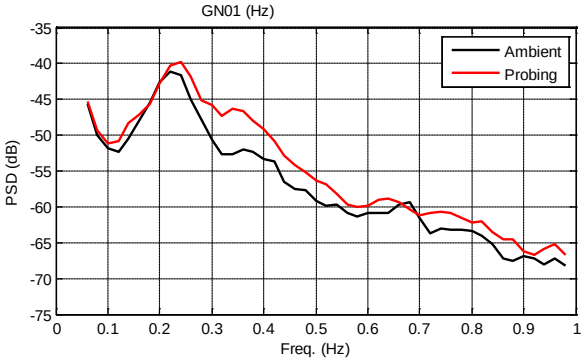

Fig. 13: Spectrum of Genesee FreqLFD during Aug. 23, 2012 probing test B.

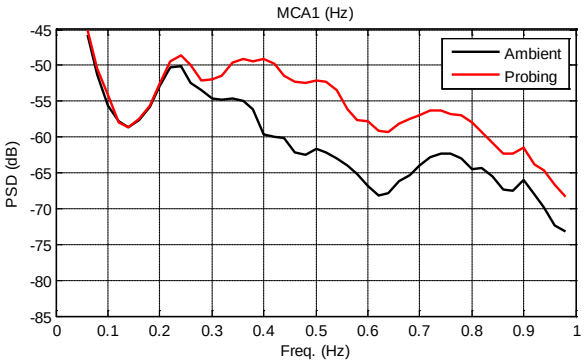

Fig. 14: Spectrum of Mica FreqLFD during Aug. 23, 2012 probing test B.

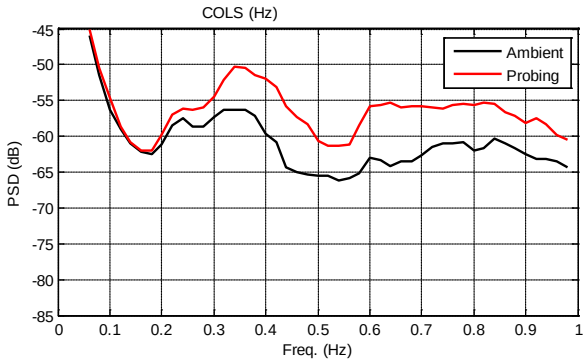

Fig. 15: Spectrum of Colstrip FreqLFD during Aug. 23, 2012 probing test B.

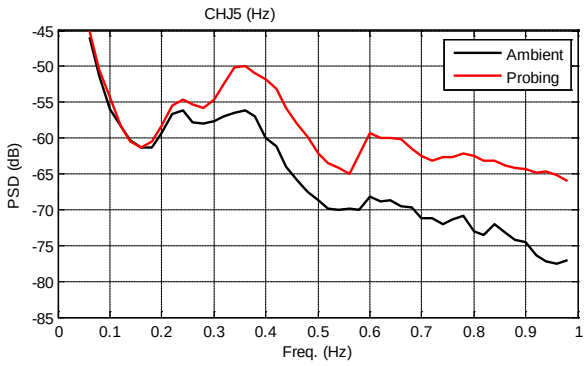

Fig. 16: Spectrum of Chief Jo FreqLFD during Aug. 23, 2012 probing test B.

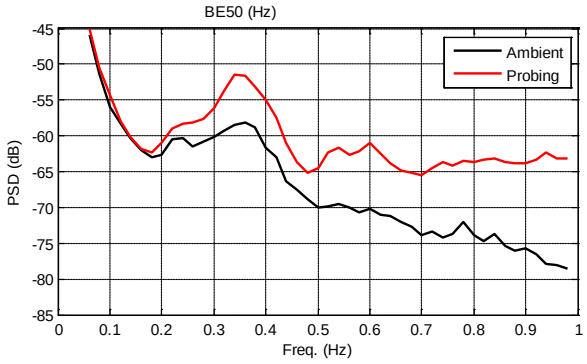

Fig. 17: Spectrum of Big Eddy FreqLFD during Aug. 23, 2012 probing test B.

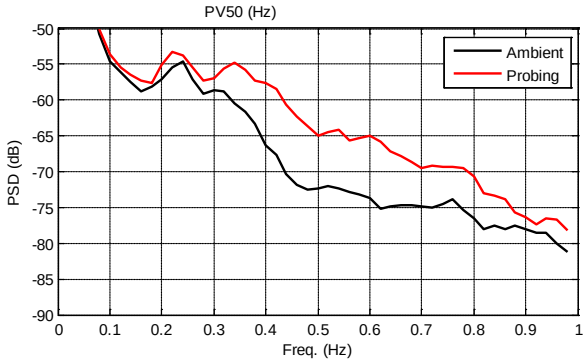

Fig. 18: Spectrum of Palo Verde FreqLFD during Aug. 23, 2012 probing test B.

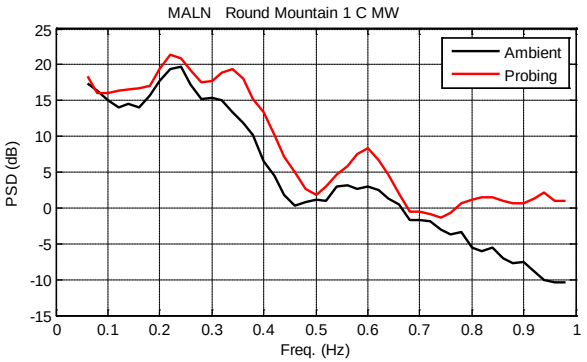

Fig. 19: Spectrum of Malin-Round M. 1 MW during Aug. 23, 2012 probing test B.

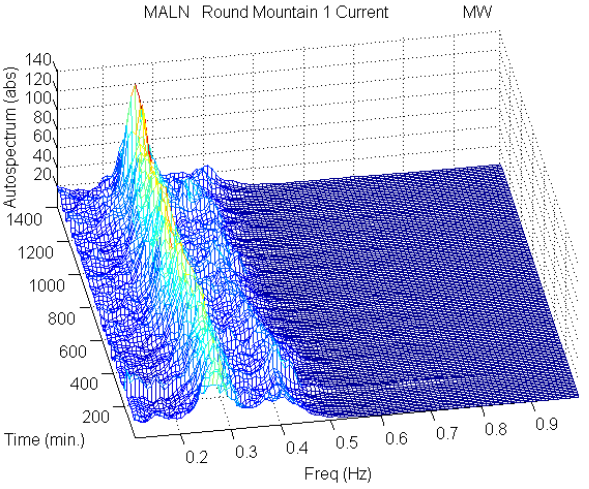

Fig. 20: Waterfall Spectrum of Malin-Round M. 1 MW during June 1, 2008.

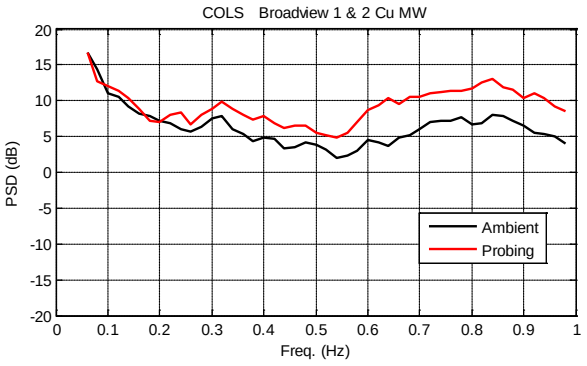

Fig. 21: Spectrum of Colstrip MW during Aug. 23, 2012 probing test B.

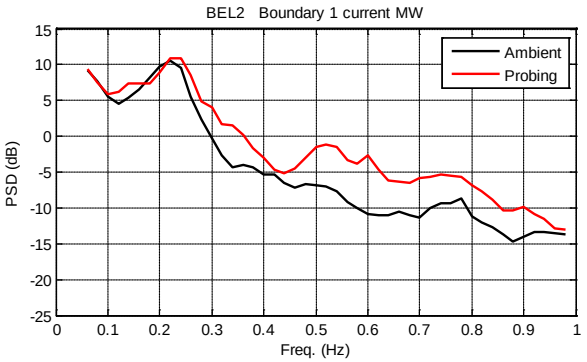

Fig. 22: Spectrum of Bell-Boundary MW during Aug. 23, 2012 probing test B.

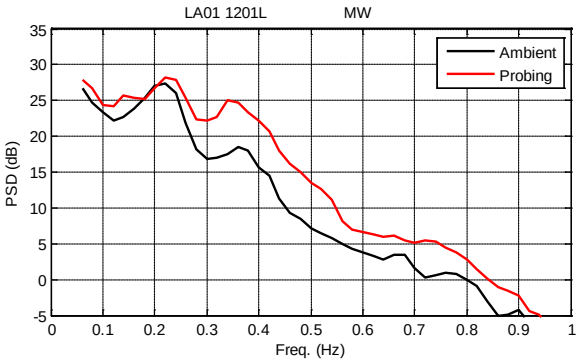

Fig. 23: Spectrum of Alberta-BC MW during Aug. 23, 2012 probing test B.

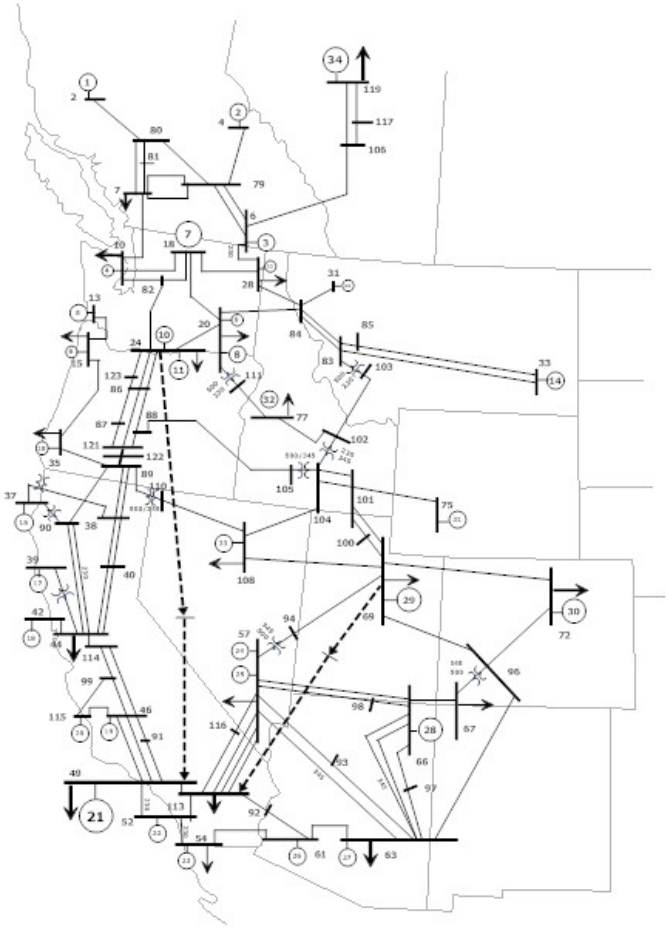

Fig. 24: High-voltage buses and lines of miniWECC model.

Table 1: miniWECC inter-area modes versus power flow cases. F = mode freq. in Hz. D = mode percent damping (100*damping ratio).

Mode	Case 1 Heavy COI Flow		Case 2 Alberta Disconnected with Reduced COI Flow		Case 3 Increased Alberta Import		Case 4 BC Importing from BPA		Case 5 So. Cal to No. Cal Flow		Case 6 So. Cal to No. Cal Flow		Case 7 So. to No. COI Flow	
	F	D	F	D	F	D	F	D	F	D	F	D	F	D
Mode A	0.211	8.3	0.317	1.6	0.188	-4.7	0.213	5.1	0.185	-4.3	0.188	-4.2	0.194	-5.3
Mode B	0.338	-0.6			0.325	-2.1	0.349	0.3	0.316	-3.5	0.331	1.5	0.356	8.6
E-W 1	0.507	9.2	0.507	8.6	0.506	8.9	0.507	8.9	0.502	9.5	0.505	9.2	0.505	7.6
Montana	0.545	7.3	0.551	7.5	0.549	8.1	0.567	8.2	0.542	7.9	0.549	8.2	0.555	7
BC	0.619	4.7	0.617	4.8	0.607	4.1	0.644	6.3	0.599	3.7	0.600	3.6	0.630	5.7
E-W 2	0.686	5.8	0.686	5.6	0.684	5.7	0.685	5.7	0.679	5.9	0.682	5.77	0.686	5.4

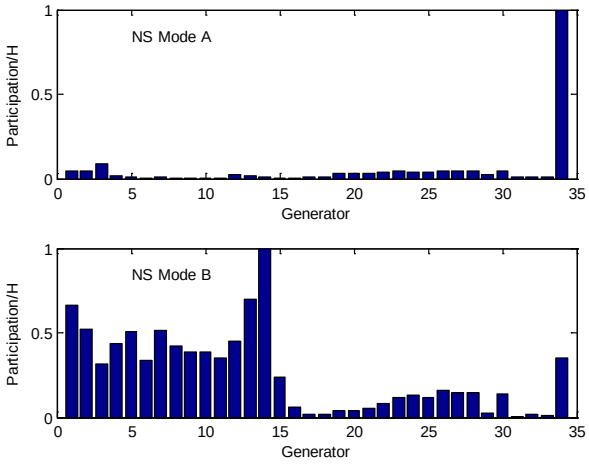

Fig. 25: NS Modes A and B participation factors for power-flow case 4 of the miniWECC model.

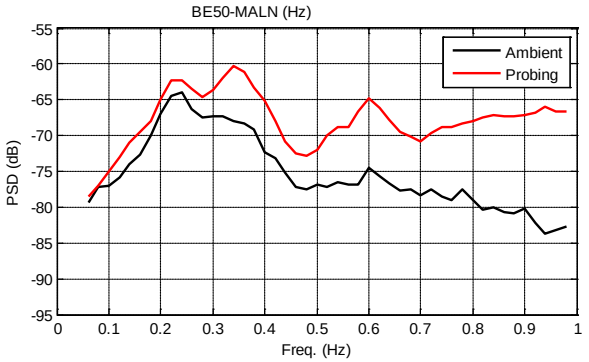

Fig. 26: Spectrum of Big Eddy - Malin FreqLFD during Aug. 23, 2012 probing test B

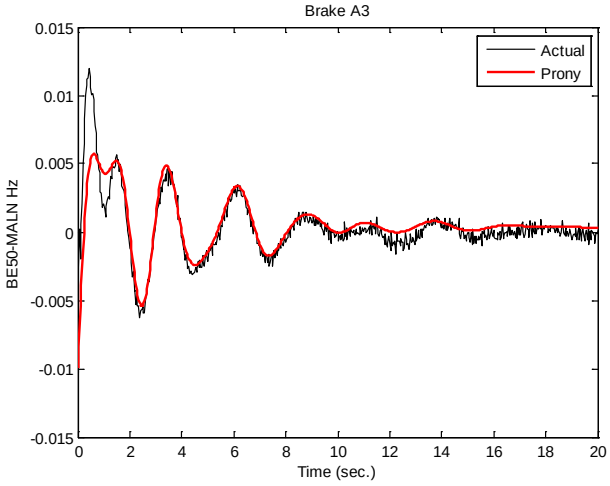

Fig. 27: Prony fit to Sep. 15, 2011 brake pulse A3, Big Eddy - Malin FreqLFD Hz.

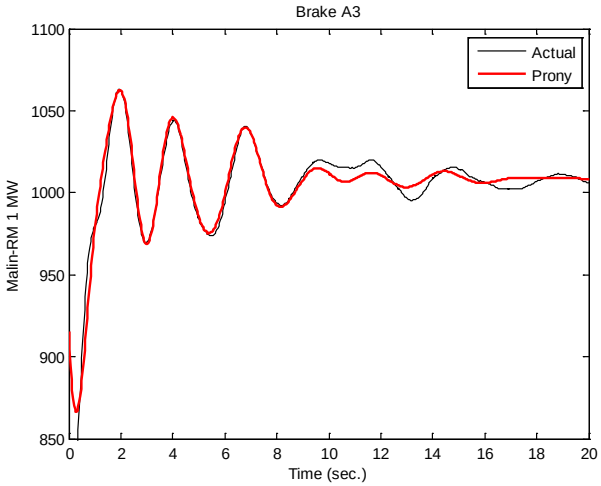

Fig. 28: Prony fit to Sep. 15, 2011 brake pulse A3, Malin-RM 1 MW.

Table 2: Modal amplitudes (or residues) from Fig. 27 and Fig. 28.

Amplitude	NS Mode A 0.261 Hz, 12.5%D	NS Mode B 0.391 Hz, 11.2%D	BC Mode 0.657 Hz, 11.1 %D
BE50-MALN (Hz)	0.00151	0.00563	0.00365
Malin-RM 1 MW	22.3	62.6	21.2

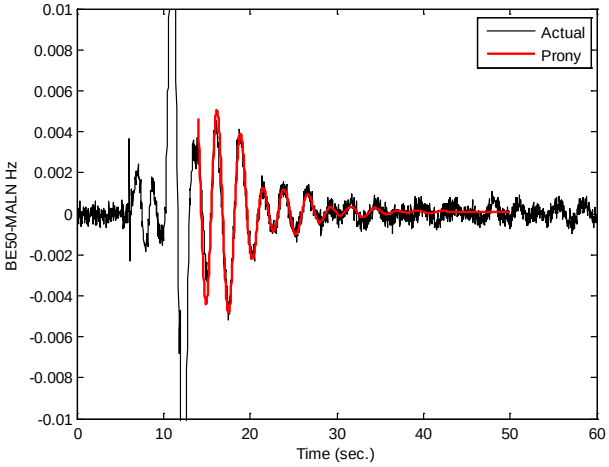

Fig. 29: Prony fit to July 4, 2012 Palo Verde event, Big Eddy - Malin FreqLFD Hz.

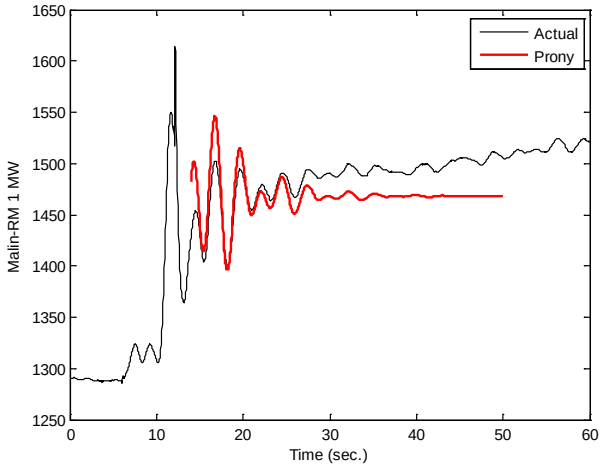

Fig. 30: Prony fit to July 4, 2012 Palo Verde event, Malin-RM 1 MW.

Table 3: Modal amplitudes (or residues) from Fig. 29 and Fig. 30.

Amplitude	NS Mode A	NS Mode B
	0.257 Hz, 10.5%D	0.386 Hz, 8.0%D
BE50-MALN (Hz)	0.0131	0.0586
Malin-RM 1 MW	331	756

IX. Conclusions

This paper summarizes the modal properties of the dominant inter-area modes in the wNAPS. These modes are the NS Mode A and the NS Mode B. The properties are estimated based upon several years of actual-system data analyses and to a lesser extent, model-based analysis. Modal properties include:

- NS Mode A is typically near 0.25 Hz. Its damping is typically larger than NS Mode B with typical damping near 10% to 15%.
- NS Mode B is typically in the 0.35 Hz to 0.4 Hz range with a damping of 5% to over 10%.
- The shape for NS Mode A has the northern half of the wNAPS swinging against the southern half. By far, the most dominant observability point is the Alberta Canada area of the system. The node or dividing line very close to Malin on the COI.
- The shape for NS Mode B has the Alberta area swinging against BC and the northern US which in turn swings against the southern part of the US. The northern node or dividing line is just south of Langdon on the BC/Alberta intertie. The other node is typically south of Tesla and north if Diablo Canyon. The observability is much more widespread than NS Mode A in that no one location is dominant.
- The controllability of NS Mode A is dominated by Alberta while the controllability of NS Mode B is very wide spread. Therefore, contingencies outside Alberta primarily excite NS Mode B.
- The Alberta-BC intertie is the largest impact on the two modes. When Alberta disconnects, the two modes "melt" into one mode typically near 0.32 Hz. This mode typically is more lightly damped. The shape for this mode is very similar to NS Mode B excluding the Alberta area PMUs.

X. Acknowledgment

The author gratefully acknowledges the many years of collaboration with Dr. John Hauer, Mr. Bill Mittelstadt, Dr. Dmitry Kosterev, Dr. Matt Donnelly, Dr. John Undrill, and Dr. John Pierre related to wNAPS dynamics and analysis methods.

XI. References

[1] D. N. Kosterev, C. W. Taylor, and W. A. Mittelstadt, "Model Validation for the August 10, 1996 WSCC System Outage," *IEEE Trans. On Power Systems*, vol. 14, no. 3, pp. 967-976, Aug. 1999.

[2] D. Trudnowski and J. Pierre, "Signal Processing Methods for Estimating Small-Signal Dynamic Properties from Measured Responses," Chapter 1 of Inter-area Oscillations in Power Systems: A Nonlinear and Nonstationary Perspective, ISBN: 978-0-387-89529-1, Springer, 2009..

[3] G. Rogers, *Power System Oscillations*, Kluwer Academic Publishers, Boston, 2000.

[4] F. L. Pagola, I. J. Perez-Arriaga, and G. C. Verghese, "On Sensitivities, Residues, and Participations: Applications to Oscillatory Stability Analysis and Control," *IEEE Transactions on Power Systems*, vol. 4, no. 1, pp. 278-285, Feb. 1989.

[5] J. F. Hauer, "Emergence of a New Swing Mode in the Western Power System," *IEEE Trans. On Power Apparatus and Systems*, vol. PAS-100, no. 4, pp. 2037-2045, April 1981.

[6] J. F. Hauer, W. A. Mittelstadt, K. E. Martin, J. W. Burns, and Harry Lee in association with the Disturbance Monitoring Work Group of the Western Electricity Coordinating Council, "Integrated Dynamic Information for the Western Power System: WAMS Analysis in 2005," Chapter 14 in the *Power System Stability and Control volume of The Electric Power Engineering Handbook*, 2nd Ed., L. L. Grigsby ed., CRC Press, Boca Raton, FL, 2007.

[7] D. Trudnowski and T. Ferryman, "Modal Baseline Analysis of the WECC System for the 2008/9 Operating Season," Final Report to Pacific Northwest National Lab, Sep. 2010.

[8] D. Trudnowski, "Baseline Damping Estimates," Appendix 4 of J. Undrill and D. Trudnowski, "Oscillation Damping Controls," Year 1 report of BPA contract 37508, Sep. 2008.

[9] D. Trudnowski, "Transfer Function Results from the 2009 and 2011 PDCI Probing Tests," Year 4 report of BPA contract 37508, Sep. 2011.

[10] D. Trudnowski, "2012 PDCI Probing Tests," Year 6 report of BPA contract 37508, Sep. 2012.

[11] D. Trudnowski, "The MinniWECC System Model," Appendix 2 of J. Undrill and D. Trudnowski, "Oscillation Damping Controls," Year 1 report of BPA contract 37508, Sep. 2008.

[12] D. Trudnowski, "Modal and Controllability Analysis of the MinniWECC System Model," Year 2 report of BPA contract 37508, Sep. 2009.

XII. Appendix 1: Theoretical BackGround

A. Theory and Definition of Modal Terms

Consistent with power-system dynamic theory [3], we assume that a power system can be linearized about an operating point. The underlying assumption is that small motions of the power system can be described by a set of ordinary differential equations of the form

$$\begin{aligned} \dot{\underline{x}}(t) &= A\underline{x}(t) + B\underline{u}_E(t) \\ \underline{y}(t) &= C\underline{x}(t) + D\underline{u}_E(t) \end{aligned} \quad (1)$$

where vector $\underline{x}$ contains all system states including generator angles and speeds, and t is time. Note that variables with an underline are vectors. System inputs are represented by the exogenous input vector $\underline{u}_E$. Measurable signals are represented by $\underline{y}$.

Define the eigen-terms for the system in (1) as

$$A\underline{u}_i = \lambda_i \underline{u}_i \tag{2a}$$

$$\underline{v}_i A = \lambda_i \underline{v}_i \tag{2b}$$

$$\underline{v}_i \underline{u}_i = 1 \tag{2c}$$

$$\underline{v}_i \underline{u}_j = 0 \text{ , for } i \neq j \tag{2d}$$

where

A = state matrix,
$\underline{u}_i$ = nx1 ith right eigenvector,
$\underline{v}_i$ = 1xn ith left eigenvector, and
λ_i = ith eigenvalue.

Define

$$U = \begin{bmatrix} \underline{u}_1 & \cdots & \underline{u}_n \end{bmatrix} \tag{3a}$$

$$V = \begin{bmatrix} \underline{v}_1 \\ \vdots \\ \underline{v}_n \end{bmatrix} \tag{3b}$$

and note that

$$UV = VU = I \tag{3c}$$

where I is the nxn identity matrix.

Modal properties are described by an eigenvalues and eigenvectors. A given mode oscillates at the imaginary part of the eigenvalue (rad/s) and the damping is defined by the eigenvalue's damping ratio (%). Mode shape is described by the right eigenvector of the A matrix corresponding to a generators speed variable. Let $\underline{u}_{i,k}$ = the kth element of the ith right eigenvector; $\underline{u}_{i,k}$ provides the critical information on the ith mode (eigenvalue) in the kth state. The amplitude of $\underline{u}_{i,k}$ is the weight for the magnitude of mode i in state x_k. It is a direct measure of the **observability** of the mode in the state. The angle of $\underline{u}_{i,k}$ provides the relative phasing of mode i in state $\underline{x}_k$. By comparing the $\angle \underline{u}_{i,k}$ for a common generator state (such as the speed), one can determine phasing of the oscillation for the ith mode. As such, $\underline{u}_i$ has been termed the "**mode shape**." For the results presented in this paper, all mode shapes are normalized to the largest term in the vector $\underline{u}_i$.

Although the right eigenvector provides critical information on the observability of a mode, it does not provide information on the controllability of the mode. **Controllability** is best described by the **participation factor**. Participation factor is the sensitivity of a mode to a given state variable and is calculated from the left and right eigenvectors. It is common to select a generator's speed state.

The participation factor for eigenvalue (mode) i and state k is defined to be

$$p_{ik} = \underline{v}_{ik} \underline{u}_{ik} \tag{4}$$

where $\underline{v}_{ik}$ is the kth element of $\underline{v}_i$, and $\underline{u}_{ik}$ is the kth element of $\underline{u}_i$. The participation factor can be interpreted using the feedback system in Fig. 31. As shown in [4], the sensitivity of the eigenvalue to the feedback gain is then

$$\frac{d\lambda_i}{dK} = p_{ik} \tag{5}$$

Equation (5) is the foundation for determining which generators with PSS units will dampen a give mode the most. For example, assume $\underline{x}_k$ is the speed state of a generator. Basically, **the equation tells us that the vector of departure in the root locus is equal to the participation factor when controlling the speed state of a generator through the torque on the shaft**. In this sense, it is a direct measure of the controllability for the generator associated with state k on mode i. The magnitude of p_{ik} is the rate at which the locus leaves the open-loop pole and the angle of p_{ik} is the angle of departure. Effectively, the participation factor is a measure as to how well control on a given generator can relatively dampen a given mode.

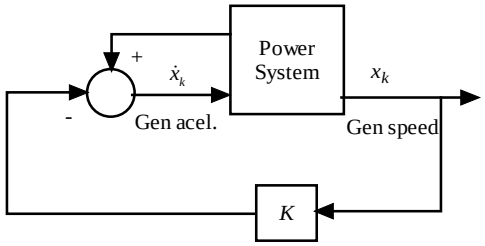

Fig. 31: Feedback system perspective of participation factors.

The participation factors are typically normalized by the inertia constant (H) of the machine scaled to a common system base.

Electromechanical modes are typically classified as "local" or "inter-area." Local modes have a single generator or power-plant oscillating against the system. An inter-area mode has several generators swinging in phase against several other generators.

B. A simple example

As a simple example, consider the system in Fig. 32. The system has three electromechanical modes described in Table 4. Mode 2 is a local mode that has generators 1 and 2 swinging against each other. Similarly, Modes 3 is a local mode that has generators 3 and 4 swinging against each other.

Mode 1 is an "inter-area" mode. The mode shape is shown in Table 5. The table clearly indicates that for mode 1, generators 1 and 2 swing together against generators 3 and 4. Also, for a given disturbance, generators 1 and 2 will have approximately double the amplitude of swing at the 0.51-Hz mode.

This is demonstrated with the simple transient simulation shown Fig. 33. Note at the lower frequency movement in the system's response at 0.51 Hz. Generators 1 and 2 move together while generators 3 and 4 swing together 180 degrees out of phase from generators 1 and 2. Also note that generators 1 and 2 have roughly double the amplitude of movement at the 0.51 Hz mode.

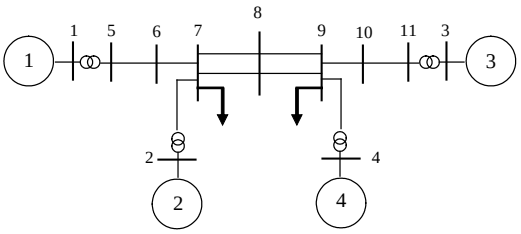

Fig. 32: Simple 4-machine example system.

Table 4: 4-machine modes.

Mode	Frequency (Hz)	Damping (%)
1	0.51	7.80
2	1.19	3.40
3	1.22	3.30

Table 5: 0.51-Hz 4-machine mode shape.

Gen	Angle($u_{i,k}$) (degrees)	Amplitude $\lvert u_{i,k} \rvert$
3	-180	1.00
4	-180	0.84
1	0	0.42
2	0	0.31

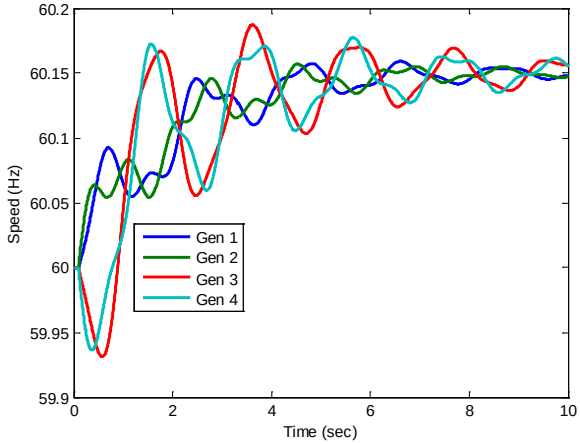

Fig. 33: Transient simulation for 4-machine system.